Official journal of the JHL 2689-9620
www.light-am.com

Article Open Access

Material removal model of magnetorheological finishing based on dense granular flow theory

Yang Bai[1,*], Xuejun Zhang[1,*], Chao Yang[2], Longxiang Li[1] and Xiao Luo[1]

Abstract

Magnetorheological finishing (MRF) technology is widely used in the fabrication of high-precision optical elements. The material removal mechanism of MRF has not been fully understood because MRF technology involves the integration of electromagnetics, contact mechanics, and materials science. In this study, the rheological properties of the MR polishing fluid in oscillation model have been investigated. We propose that the shear-thinned MR polishing fluid over the polishing area should be considered a dense granular flow, based on which a new contact model of MRF over the polishing area has been constructed. Removal function and processing force test experiments were conducted under different working gaps. The normal pressure and effective friction equations over the polishing area were built based on the continuous medium and dense granular flow theories. Then, a novel MRF material removal model was established. A comparison of the results of the theoretical model with actual polishing results demonstrated the accuracy of the established model. The novel model proposed herein reveals the generation mechanism of shear force over a polished workpiece and realizes effective decoupling of the main processing parameters that influence the material removal of MRF. The results of this study will provide new and effective theoretical guidance for the process optimization and technology improvement of MRF.

Keywords: Magnetorheological finishing, Material removal mechanism, Dense granular flow, Removal function, Optical fabrication

Introduction

Magnetorheological finishing (MRF) has been widely used in the ultra-precision fabrication of plane, spherical, aspherical, and some free-form optical elements[1–4]. A variety of materials can be polished up to the nanometer level with MRF. The surface accuracy and quality after MRF can satisfy the requirements of optical systems used in industrial, high-power lasers, medical or semiconductor optics[5,6]. It is known that MRF technology involves the interdisciplinary of electromagnetics, chemistry, rheology, and contact mechanics. The shear force generation mechanism during the polishing process and have not been elucidated and the present material removal model is not instructive enough for the study of MRF.

Extensive research has been conducted to reveal the material removal mechanism of MRF. A.B. Shorey adopted Bingham fluid model and proposed that material removal depends on the shear stress over the workpiece based on the fluid lubrication theory[7]. This is a preliminary study on the MRF material removal mechanism. Kordonski built a material removal model based on the Preston equation by introducing a modified Preston coefficient[8]. The established model shows the relationship between the material removal rate and normal force, which depends on

Correspondence: Yang Bai (baiyang5406@sina.com) or Xuejun Zhang (zxj@ciomp.ac.cn)
[1]Key Laboratory of Optical System Advanced Manufacturing Technology, Changchun Institute of Optics, Fine Mechanics and Physics, Chinese Academy of Sciences, Changchun 130033, China
[2]Changchun University of Science and Technology, Changchun, Ji Lin, 130022, China

the friction coefficient and normal pressure on the workpiece during the polishing process. They proposed that the normal force and shear stress over the workpiece during the polishing process arise from the hydrodynamic pressure between the polishing fluid and the workpiece.

However, A. B. Shorey discovered that the hydrodynamic pressure of the polishing powder during processing is too low to achieve efficient material removal and proposed that the material removal efficiency is proportional to the shear stress on the workpiece, in subsequent research[9]. Lambropoulos reported that material removal efficiency is linearly related to the mechanical properties (grinding figure of merit) of the polished materials[10]. DeGroote built a material removal rate model for glasses by carrying out large numbers of experiments[11]. The model covers the effects on the material removal rate of the concentration and size of the iron powders and abrasives used in the MR polishing fluid, the processing force on the workpiece surface, the pH of the fluid, the mechanical parameters of the polished material, and the surface energy. However, there is still a large deviation between the model and the experimental results considering only the peak removal rate. Therefore, the established model cannot be applied to predict the MRF material removal rate. Miao used the spot taking machine (STM) to study the process force on a workpiece during the MRF process[12,13]. The normal pressure and shear force on the workpiece in polishing BK7 glass and alumina nitride ceramics (ALON) were measured under different process conditions. It was also found that the material removal rate was approximately linear with the shear stress on the workpiece, the friction coefficient in polishing ceramics was basically constant, and the friction coefficient in polishing glass was variable, but the reason was not clear. The generation mechanism of the shear force during polishing was not presented. Kordonsiki proposed that the force generating the material removal of MRF is due not to the hydrodynamic pressure from the MR polishing fluid, but to the severe collision of iron powder particles and abrasives in the polishing area, which resulted in a large shear force over the contact area of the workpiece surface[14]. Markus Schinhaerl established a mathematical model for the MRF removal function based on the contact model and removal function experiments. The model can predict the removal function distribution under specific process parameters[15,16]. Liu calculated the hydrodynamic pressure and built the removal function model based on Preston function[17]. Then, an interactive regionalized modeling approach of tool influence function for the processing of aspherical optics was proposed.

Previous research has demonstrated that the material removal of MRF depended on the shear stress over the workpiece in the polishing area, and the shear stress can be influenced by the composition of the MR polishing fluid and process parameters, such as the magnetic field strength, penetration depth, et al. However, the mechanical properties of the MR polishing fluid change under a high shear rate in the polishing process[18–20]. These changes arise from the microstructure breakdown of the MR polishing fluid in the converging gap, which develops into the sheared particle flow that consists of particles added to the MR polishing fluid. Meanwhile, the normal force from the unsheared core attached to the wheel will influence the sheared flow, which means that the surface abrasion (material removal rate) will be different as the normal force changes. This should be fully considered, especially in the processing of complex surfaces with MRF. Therefore, a new principle should be introduced to reveal the material removal mechanism of MRF and further optimize the process parameters and MR polishing fluid.

Based on the measurement and analysis of the rheological characteristics of the MR fluid under a high shear rate, we proposed to divide the MR polishing fluid in the polishing area into a shear thinned dense granular flow and a magnetized core that is attached to the polishing wheel without shearing. According to the removal function experiments and processing force test, a novel theoretical model of the MRF removal function was established based on the dense granular flow theory. The established model can simply realize the decoupling of the MRF processing parameters effectively. The results of this study have important theoretical significance in the research and application of MRF technology.

Rheological properties of MR polishing fluid under high shear rate

The MR polishing fluid is mainly composed of a low-viscosity base carrier (usually water), iron particles, and abrasives. The size of the iron powders used in the MR polishing fluid is 1–10 μm and the size of the abrasives is much smaller. Nanometer-sized diamond or cerium oxide is usually used depending on the processing material. In the polishing process, the MR polishing fluid is magnetized as rotating with the polishing wheel to the polishing area. The uniformly dispersed iron powders and abrasives are rearranged, showing the characteristics of a viscoplastic body under the action of a magnetic field. The shear and compression contact between the MR polishing fluid and workpiece in the polishing process results in fluid structural remodeling, and the magnetization chain of iron particles become closer and strengthened. The abrasives are separated from the magnetized MR fluid ribbon interior

to the surface under the gradient magnetic field and by scratching the workpiece surface in the polishing area, which resulted in material removal. During the polishing process, the MR polishing fluid is subjected to a high shear rate (> 500/s). Therefore, the rheological behavior of the MR polishing fluid under a high shear rate plays a key role in the material removal mechanism of MRF.

A commercial magneto-rheometer (MCR302) was used to analyze the rheological properties of the MR polishing fluid during the polishing process. The storage modulus and shear modulus under shear in the oscillation mode were investigated by adopting the commonly used MR polishing fluid. The median size of the iron particles (carbonyl iron powders) used was 4 μm and the volume content was 40%. The abrasives used in the fluid were nano-diamond, with a median size of 100 nm and a volume content of 0.1%. The base carrier liquid was deionized (DI) water. Scanning electron microscopy (SEM) images of the iron particles and nano-diamond used in the MR polishing fluid are shown in Fig. 1.

The rheological measurement conditions adopted were a magnetic field strength of 250 kA/m, an oscillation frequency of 2 Hz, a rotor diameter of 20 mm, and a distance of 1 mm between the rotor and test disk. The testing results of the storage modulus and shear modulus under dynamic oscillation mode are shown in Fig. 2. The results show that when the MR polishing fluid is subjected to a low shear rate, its storage modulus and shear modulus are approximately 0.82 and 0.95 MPa, respectively, which means that the MR fluid shows elastic properties at this state. However, when the shear strain increases, the storage modulus and shear modulus decrease sharply, which means that the shear force between the rotor and the magnetized MR fluid is greater than its shear yield stress, and the MR fluid is sheared and thinned to form a sheared granular flow with a further increase in shear rate[14].

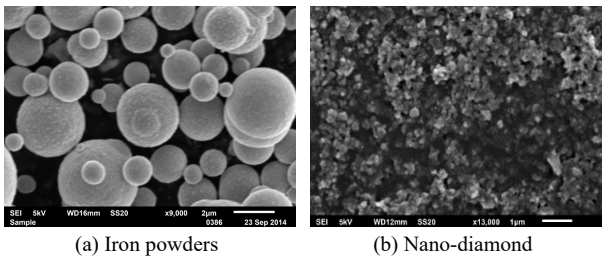

(a) Iron powders (b) Nano-diamond

Fig. 1 Scanning electron microscopy (SEM) images of iron powders **a** and abrasives **b** used in the magnetorheological (MR) polishing fluid.

However, in an actual polishing process, the MR polishing fluid in contact with the workpiece is not completely shear thinned. The rim of the magnetized MR polishing fluid in contact with the workpiece is shear thinned, but the bulk of the MR polishing fluid attached to the polishing wheel undergoes structural reconstruction under extrusion. Thus, the magnetization chains become shorter and with denser stacking, resulting in a viscoplastic body. Therefore, the rheological properties of the sheared granular flow formed by the MR polishing fluid and the properties of the unsheared magnetized solid-like body will determine the material removal rate and the removal function distribution of MRF. Therefore, it is crucial to elucidate the generation mechanism of the shear force on the workpiece, in the MRF process, and establish a theoretical model of the removal function.

Interaction between the MR polishing fluid and workpiece in the polishing area

The MR polishing fluid circulates along with the rotation of polishing wheel in the actual polishing process, and the abrasives seep from the MR polishing fluid under the magnetic field effects in the polishing area. Owing to the small distance between the polishing wheel and the

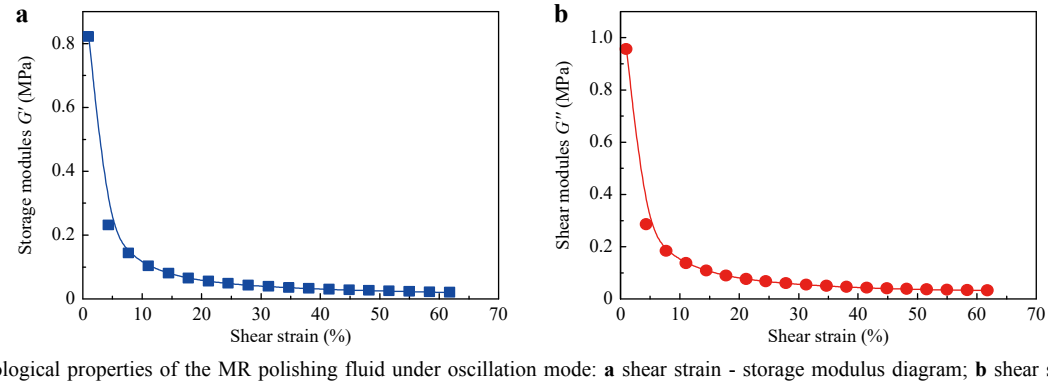

Fig. 2 Rheological properties of the MR polishing fluid under oscillation mode: **a** shear strain - storage modulus diagram; **b** shear strain - shear modulus diagram.

workpiece, the magnetized MR polishing fluid is squeezed and sheared. This effect causes the rearrangement of the magnetized structure, resulting in a wide and thin fluid ribbon. As a result, there exists a large shear force between the MR polishing fluid and the workpiece owing to the rotation of the polishing wheel, which results in the removal of material from the workpiece. Based on the rheological characteristics of the MR polishing fluid under a high shear rate and the coupling relationship of multiple parameters under the actual polishing state, we considered the sheared thinned particle flow that contacting the workpiece as a dense granular flow, whereas the unsheared magnetized solid core after extrusion and reorganization is regarded as a viscoplastic body in this study.

Concept of dense granular flow

Dense granular flows are widely used in tribology, powder metallurgy, hydropower engineering, geological hazards, and other fields[21,22]. A dense granular flow is a particle system composed of large numbers of discrete solid particles that are generally static when there is no external disturbance. However, when the system is subjected to external shear, vibration, rotation, or fluid disturbance, the system exhibits a flow phenomenon similar to that of a liquid. The dense granular system shows the rheological properties of a plastic body as a whole[23,24]. In contrast to the classical Bingham fluid or Herschel–Bulkley fluid, the special feature of a dense granular flow is that the effective viscosity depends on both the shear rate and the confining pressure. This feature is embodied in the frictional property of a granular flow medium under pressure[25,26]. Therefore, we constructed a schematic diagram of the interaction between the MR polishing fluid and the workpiece in the MRF polishing process, as shown in Fig. 3.

Based on the rheological properties of the MR polishing fluid, we divided the polishing fluid in the polishing area into two layers, as shown in Fig. 3b. The interior layer attached to the wheel, which is a magnetized solid-like core, and the outer layer of the MR polishing fluid in contact with the workpiece, which changes to a dense granular flow under the high shear rate. Under the actual polishing state, tangential sliding exists between these two layers. The magnetized solid-like core is squeezed, and the generated normal force acts upon the shear dense granular flow (which consists of iron particles, abrasives, and carrier fluid) in the polishing area. Therefore, this normal force directly influences the interaction characteristics between the granular flow and workpiece. The results are reflected in the friction characteristics at the contact interface and the shear force over the workpiece, during the polishing process[27].

Shear stress of the dense granular flow

It is known that the material removal of the MRF depends on the shear force over the workpiece surface. According to the rheological analysis and actual polishing contact model, the shear stress over the workpiece is

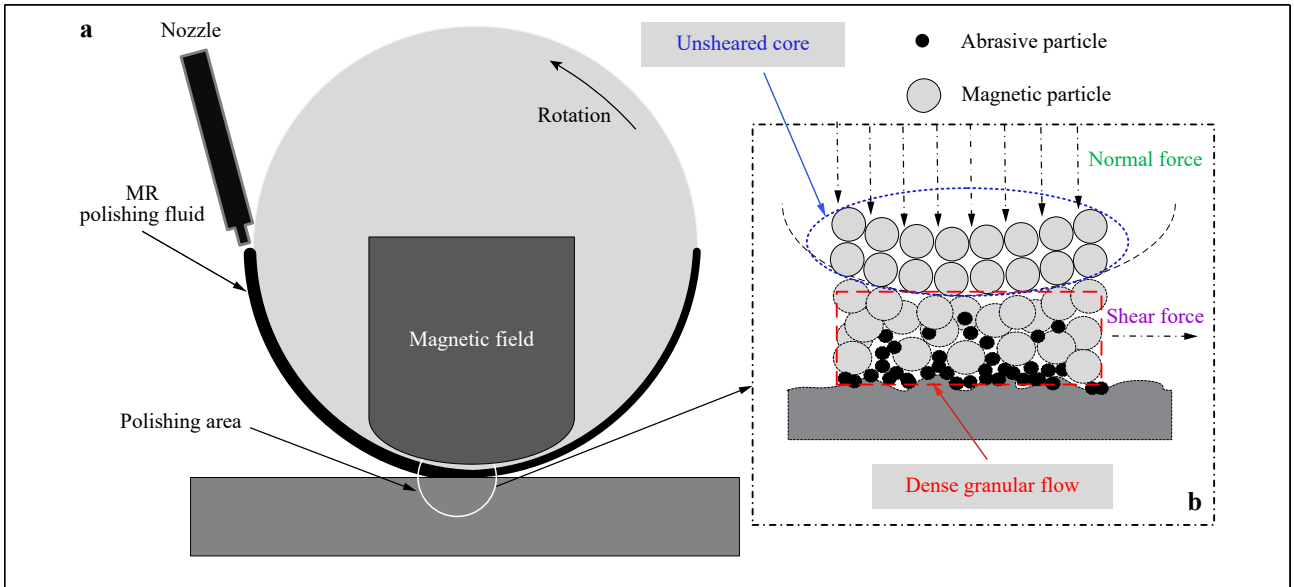

Fig. 3 The shear force generation mechanism of MRF: **a** contact model of MRF; **b** the rheological behavior and interaction of MR polishing fluid with workpiece in polishing area.

determined by the normal pressure from the unsheared magnetized core and friction over the workpiece arising from the sheared dense granular flow. The solid particles (abrasives and carbonyl iron powders) used in the MR polishing fluid are not standard frictionless spherical particles. Therefore, the shear stress can be written as shown in Eq. 1 according to the constitutive law of dense particle flow.

$$\tau = \mu(I_m)P$$

$$\mu(I_m) = \mu_0 + \beta I_m^{\alpha},\ I_m = \dot{\gamma}\bar{d}(p/\bar{\rho}_s)^{-0.5} \quad (1)$$

where τ is the shear stress, $\mu(I_m)$ is the friction coefficient, I_m is the modified inertial number of dense granular flow, α is the parameter related to the particle shape and surface properties, β is a parameter that depends on the MR fluid rheological properties, P is the pressure acting upon the dense granular flow, d and ρ_s are the average particle size and density of the particles, respectively, and $\dot{\gamma}$ is the shear rate of the granular flow. During the polishing process, the granular flow is in an equilibrium state, and the sheared thinning granular flow velocity is close to the magnetized core velocity, which is consistent with the speed of the polishing wheel. However, it is different from Preston equation, the influence of granular flow velocity on removal function is reflected through shear rate based on granular flow theory.

Therefore, corresponding to the MRF process, τ is the shear force over the workpiece surface during the polishing process, and $\mu(I_m)$ is the effective friction coefficient of the interface between the MR polishing fluid and the workpiece over the polishing area. P is the normal pressure on the granular flow formed by the sheared thinning MR polishing fluid. P depends on the mechanical and rheological properties of the MR polishing fluid under squeezing and shear after magnetization. Therefore, it is necessary to acquire the normal pressure distribution and effective friction coefficient over the workpiece to build a shear stress model and material removal model of the MRF.

Normal force over polishing area

As a result, the MR fluid exhibits rheological properties similar to those of a viscoplastic body under a high shear rate in the polishing state. The solid-like magnetized core of the MR polishing fluid attached to the polishing wheel will be in the squeeze state in an unlimited space. Considering that the magnetic field in the polishing area is not a uniform magnetic field, we analyzed the normal force under the magnetic field with a magnetorheometer (MCR-302) because the magnetic field intensity distribution of the MR testing module is close to the magnetic field generation module of the MRF. Therefore, it can accurately reflect the normal force characteristics of the MR polishing in the actual polishing process. According to the typical process parameters presented in Table 1, the normal force characteristics of the MR fluid under different shear rates were tested using a magnetorheometer, and the results are shown in Fig. 4.

The normal force of the MR fluid gradually increases under a low shear rate. However, when the shear rate exceeds 0.3/s, the MR fluid contacting the moving wall exhibits solid–liquid conversion and solid particle rearrangement, which results in a gradual decrease in the normal pressure. As the shear rate increases further, the normal force gradually decreases and tends to the initial normal force, which is quasistatic. Thus, the normal force from the unsheared solid-like core in the MRF process can be expressed based on the continuous media theory [28,29].

Therefore, the force acting on the sheared thinning MR polishing fluid can be expressed as shown in Eq. 2 according to the polishing parameters and fluid rheological properties.

$$F_N = \frac{a}{h^{n-1}} - \frac{b}{h^n} + \delta \quad (2)$$

where a and b are coefficients that depend on the volume and shear yield stress of the MR polishing fluid, h is the gap distance, and δ is the modification parameter of F_N under a non-uniform magnetic field. The parameter n is determined by the rheological properties of the MR polishing fluid, magnetic field strength, and polishing parameters. Based on the MRF process contact model shown in Fig. 5, h_1 is the initial thickness of the MR fluid

Table 1 Typical process parameters

Parameters	Wheel diameter/mm	Rotate speed/(r/min)	Rate of flow/(ml/min)
Value	160	120	480

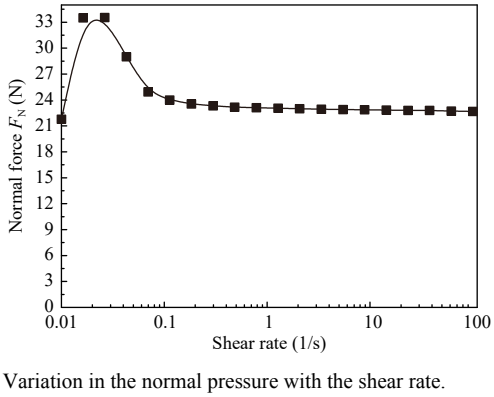

Fig. 4 Variation in the normal pressure with the shear rate.

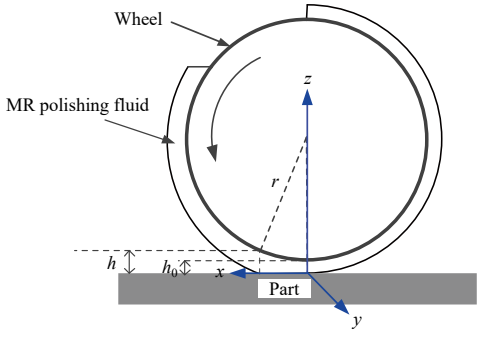

Fig. 5 Contact model diagram of polishing process.

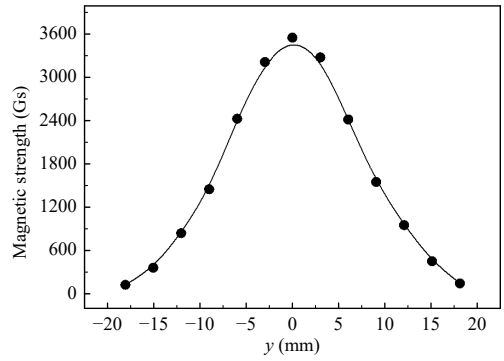

Fig. 6 Magnetic strength and distribution over the polishing wheel surface along the y direction.

ribbon before contact with the workpiece, and h_0 is the thickness after exiting from the polishing area. R is the radius of the polishing wheel.

Therefore, the normal force F_N along the x-coordinate can be approximately expressed by the following equation:

$$F_N = \frac{a}{\left(h_0 + \frac{x^2}{2R}\right)^{n-1}} - \frac{b}{\left(h_0 + \frac{x^2}{2R}\right)^{n}} + \delta \tag{3}$$

Effective friction over the contact area

According to the dense granular theory, the effective friction over the contact area depends on the normal pressure, particle size distribution, density, and shear rate. The magnetic confinement pressure of MRF is different from that of a regular sheared granular flow. Removal function experiments were carried out with self-developed MRF polishing machine based on permanent magnetic generator. The gradient magnetic strength and distribution over the polishing wheel surface along the y direction according to the contact model (Fig. 5) is shown in Fig. 6

The process force is measured with the Kistler force sensor, and the spot area and removal rate were calculated based on the testing results with interferometry. The process parameters are presented in Table 1.

According to the previous experimental results, the initial MR fluid ribbon height, corresponding to h_1 shown in Fig. 5, was 2.0 mm with the typical processing parameters. The normal force, shear force, and removal function area under different working gaps h_0 were measured through a removal function experiment with BK7 glass. The results are presented in Table 2.

The normal force depends on the working gap and has a decisive influence on the inertial number of a granular flow consisting of a sheared thinned MR polishing fluid in the polishing area. According to the results listed in Table 2, Fig. 7 shows the normal pressure under different working gaps and the fitting results with Eq. 2. This result also demonstrates the pressure along the long axis of the removal function owing to the changes in penetration depth.

According to the fitting results, we can obtain the coefficients a = 292, b =85, and n = 5, $\delta \approx 0$. The R-square (coefficient of determination) is 0.9992 and the RMSE (root mean squared error) is 17.75 with the fitting equation. Considering the MR polishing fluid composition and properties, the coefficient α can approximate to 1 for a sheared granular flow in the polishing area based on the granular flow theory and the effect of shape and friction of particles of the granular flow. Therefore, the modified inertial number I_m in Eq. 1 can be simplified as follows:

$$\mu = \mu_0 + AP^{-0.5}, \quad A = \beta \frac{\dot{\gamma}\bar{d}}{\sqrt{k\bar{\rho}_s}} \tag{4}$$

Based on Eq. 4 above and the friction results listed in Table 2, we can obtain the fitting results of friction under

Table 2 Effect of working gap on processing force and spot area

working gap/mm	Shear force/N	Normal force/N	Effective Friction (μ)	Spot area/mm²	Normal pressure/kPa
1.1	3.2 ± 0.05	6.7 ± 0.05	0.48	44.5 ± 0.5	150
1.3	1.92 ± 0.05	3 ± 0.05	0.64	36.5 ± 0.5	83
1.5	0.94 ± 0.05	1.3 ± 0.05	0.72	27.3 ± 0.5	47.6
1.7	0.54 ± 0.02	0.64 ± 0.02	0.84	18 ± 0.5	35.16
1.9	0.12 ± 0.01	0.12 ± 0.01	1	6 ± 0.2	20

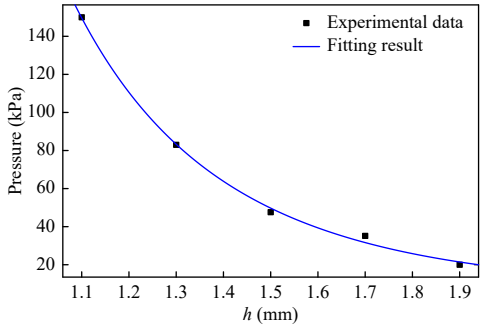

Fig. 7 Normal pressure under different working gaps.

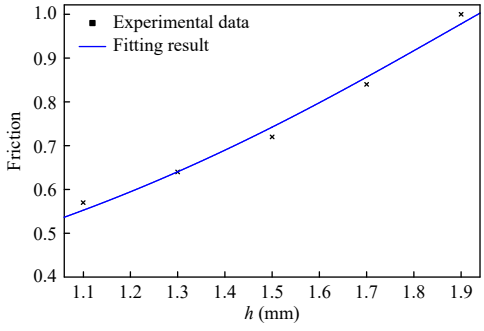

Fig. 8 Effective friction under different working gaps.

different working gaps, as shown in Fig. 8. The fitting results show that μ_0 = 0.38 and A = 2. The R-square (coefficient of determination) is 0.991 and the RMSE (root mean squared error) is 0.0165 with the fitting Eq. 4. These results demonstrate the effective friction under different working gaps during MRF process.

Abrasive concentration over the polishing area

As shown in Fig. 3, there is a division of the filler particles under the magnetic impact in the polishing area: magnetic particles are attracted to the polishing wheel, and abrasive particles are gathered in the surface layer. The removal of material is due to the cutting of the surface roughness by the sharp edges of abrasives moving with the MR polishing fluid. Therefore, the abrasive concentration over the polishing area affects the material removal rate and removal function profile. The concentration distribution of dispersed particles of the MR polishing fluid in the gap between the workpiece and polishing wheel can be simulated based on the Boltzmann law[30]. The abrasive particle number N_c in the sheared layer along x under typical process parameters can be expressed as follows:

$$N_c(x) = N_a \frac{1 - exp\left[-m_a g_a h\left(\frac{2\eta t_r}{3n}\dot{\gamma}^2\right)^{-1}\right]}{1 - exp\left[-m_a g_a((R+h_1)-h)\left(\frac{2\eta t_r}{3n}\dot{\gamma}^2\right)^{-1}\right]} \quad (5)$$

where N_a is the abrasive concentration of the MR polishing fluid, m_a is the mass of the abrasive particle, and g_a is the acceleration of the motion of the abrasive particles under the influence of the magnetic volume force. R is the radius of the polishing wheel, η is the viscosity of the base MR base fluid, $\dot{\gamma}$ is the shear rate, t_r is the relaxation time, and n is the number of abrasive particles in the contact bulk over the polishing spot.

The number of abrasive particles that contact the workpiece is also influenced by the removal function spot shape. The shape parameter of a typical MRF removal function is shown in Fig. 9. The length and width of the removal function are a and b, respectively, and the outer contour of the removal function is approximately parabolic.

Therefore, the outer contour of removal function can be expressed as follows:

$$y = \sqrt{\frac{a^2}{4b}(b-x)} \quad (6)$$

Based on Eq.5, 6, we can obtain the abrasive particle concentration C_a along the long axis of the removal function:

$$C_a = N_a \frac{1 - exp\left[-m_a g_a\left(h_0 + \frac{x^2}{2R}\right)\left(\frac{2\eta t_r}{3n}\dot{\gamma}^2\right)^{-1}\right]}{1 - exp\left[-m_a g_a\left((R+h_1) - \left(h_0 + \frac{x^2}{2R}\right)\right)\left(\frac{2\eta t_r}{3n}\dot{\gamma}^2\right)^{-1}\right]} \left(\frac{a^2}{4b}(b-x)\right)^{-\frac{1}{2}} \quad (7)$$

Material removal model of MRF

It is known that the MRF material removal rate depends on the shear stress over the polishing area. In contrast to

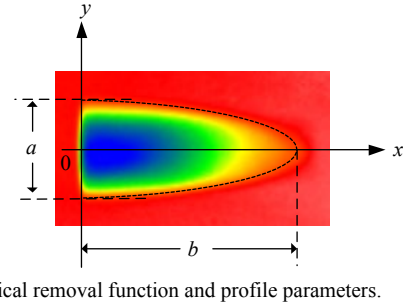

Fig. 9 Typical removal function and profile parameters.

the traditional Preston equation, the normal pressure is substituted by shear stress over the polishing area, and the polishing velocity is considered as an impact factor on the inertial number in this study. The shear stress calculated based on the granular flow decouples the complex influence parameters on the MRF material rate from a new perspective. Thus, the MRF material removal model can be expressed as follows:

$$MRR = C\tau = C_{MRF}\mu F_N \tag{8}$$

C_{MRF} is the coefficient of the theoretical material removal rate based on the granular theory. The parameter C_{MRF} is mainly determined by the mechanical merits of the workpiece, abrasive concentration, particle size distribution, and properties. In this study, we focus on the profile of the removal function from the inlet to the lowest point of the MR fluid ribbon under the wheel (from 0 to b), which can reveal the material removal mechanism and the main factors influencing the MRF process. Therefore, we can obtain the novel material removal model based on Eq. 3, 4, 7, 8, and the material rate of MRF along x (long axis) can be expressed as Eq. 9.

Under the typical polishing parameters, h_0 = 1 mm, the polishing wheel radius R = 80 mm, and the removal function size coefficients $a \approx 6$ mm and $b \approx 13$ mm. The iron particle used in the MR polishing fluid is carbonyl iron with a density $\rho_m = 7.5 \times 10^3$ kg/m^3, average magnetization $J_m = 5 \times 10^5$ A/m, and median size of $d = 2 \times 10^{-6}$ m. The abrasive particles used in the MR polishing fluid are nano-diamond with a volume concentration of 0.1 vol%, the particles of which have a density $\rho_a = 3.5 \times 10^3$ kg/m^3 and median size of 100 nm. The shear rate $\dot{\gamma}$ exceeds 500/s in the steady shearing state during the polishing process with the typical process parameters, according to the contact model of the MRF proposed in this study. Therefore, we adopted $\dot{\gamma}$ = 1000/s and relaxation time $t_r = 10^{-3}$ s. Thus, we can obtain the theoretical material removal rate along the long axis of the removal function based on the friction fitting results of pressure and friction under typical process parameters. The actual and theoretical material removal profiles along the long axis of the removal function are shown in Fig. 9, and the coefficient, C_{MRF} is approximately 0.12. The results demonstrate that the material removal model proposed in this study can depict the material removal distribution along the long axis of the MRF removal function. Moreover, the material removal model proposed here can also illustrate the deviation between the projection point of the lowest point of polishing wheel and the highest material removal of the removal function, which is also shown in Fig. 10. The deviation Δx along the long axis of the removal function is determined by the MR polishing fluid properties and process parameters. To achieve a highly determined fabrication of workpieces, this deviation should be considered in the actual polishing process.

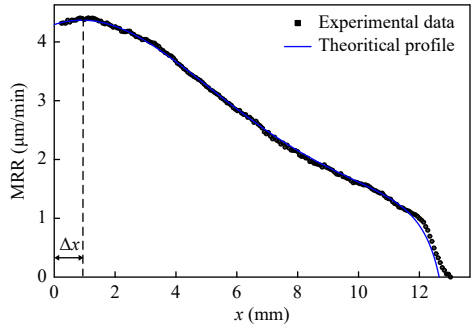

Fig. 10 Comparison of theoretical and actual polishing removal function profile along the long axis.

Discussion and conclusions

Magnetorheological finishing (MRF) is a typical multi-disciplinary processing technology, an accurate theoretical model of removal function with decoupled parameters has not been established so far. Through the research of the rheological characteristics of MR polishing fluid and the contact model of MRF process, a new mechanism to reveal the source of shear force in MRF is proposed based on the granular flow theory and a novel material removal model is established.

The established model is also based on the shear stress in the polishing process similarly to the previous studies. However, it is different from simplifying the MR polishing fluid as Newtonian fluid and calculating the shear stress based on hydrodynamics directly. The MR fluid shear modulus and storage modulus under dynamic oscillation mode are analyzed in this work. Then, the MR polishing fluid in the polishing area is divided into two layers according to the actual contact model of MRF. The upper layer is a magnetized solid-like body, whereas the lower layer is a sheared thinning dense granular flow that consists of particles and base liquid added in the fluid. The shear force generation mechanism of MRF is investigated based on the granular flow theory and the material removal model is established based on the contact model of MRF. The comparison of the theoretical and actual polishing removal function profiles along the long axis indicates that the proposed material removal model in this study can accurately describe the actual material removal along the long axis of the MRF removal function.

The model covers the main parameters that influence the material removal rate and removal function distribution.

Such parameters include magnetic field characteristics, shear rate (polishing wheel rotation speed), MR fluid viscosity and the size of added particles, removal function area, polishing wheel sizeparameters that influence the material removal function are as follows:

$$MRR(x) = C_{MRF} \frac{1 - exp\left[-m_a g_a \left(h_1 - h_0 - \frac{x^2}{2R}\right)\left(\frac{2\eta t_r}{3n}\dot{\gamma}^2\right)^{-1}\right]}{1 - exp\left[-m_a g_a \left(R + h_0 + \frac{x^2}{2R}\right)\left(\frac{2\eta t_r}{3n}\dot{\gamma}^2\right)^{-1}\right]} \left(\frac{a^2}{4b}(b-x)\right)^{-\frac{1}{2}} \left(\mu_0 F_N + \beta \frac{\dot{\gamma}\bar{d}}{\sqrt{k\rho_s}} F_N{}^{0.5}\right) \tag{9}$$

(a) The size of particles added in MR polishing fluid mainly affects the inertia parameter of the sheared granular flow, and then affects the shear force over the workpiece and the material removal rate.

(b) The magnetic field strength in the polishing area and the rotating speed of polishing wheel will determine the concentration of abrasives in the sheared granular flow and the shear force over the workpiece, then the material removal rate and the distribution of removal function will be affected.

(c) The working gap has the opposite effect on the positive pressure on the workpiece and the surface effective friction coefficient. However, the shear force will still decrease as working gap increases under the conventional processing parameters and typical MR polishing fluid composition, which is also proved by large numbers of experiments.

In general, the effects of polishing parameters on material removal rate and removal function distribution can be evaluated with the novel material removal model proposed in this work. This is very importance for the research of MRF technology. However, it is necessary to adjust the variables of the model according to the processing parameters and polished materials to improve the prediction accuracy. This is also the deficiency of the material removal model and one of the subsequent research contents.

Therefore, the main conclusions are as follows:

(1) In the MRF process, there exists the partial solid-liquid conversion of MR polishing fluid near the workpiece surface, and a sheared dense granular flow is formed between the solid-like magnetized core and the workpiece.

(2) The shear stress generation mechanism of MRF process can be investigated based on granular flow theory and the contact model of MRF.

(3) The material removal model proposed based on dense granular theory can decouple the main parameters that affect the material removal of MRF.

(4) The peak point of MRF removal function is not coincident with the maximum pressure point. It is the result of the combined effect of abrasives concentration over contact area and shear force distribution. This is particularly important for the position calibration and the control of removal function stability during actual polishing process.

The results of this study provide theoretical support for research on the mechanism and optimization of the MRF technology. The material removal model proposed in this paper is beneficial for the researchers to improve the MR polishing fluid composition and processing parameters according to the polishing requirements. Moreover, the studies of the material removal prediction and removal function distribution changes under different polishing conditions can also be targeted with the theoretical model. The proposed material removal model in this work overcomes the limitations of the traditional Preston equation to describe the material removal of MRF and will be promising for the mechanism studies and process improvement of other optical fabrication technologies.

Acknowledgements

Y. Bai and X. J. Zhang acknowledge the funding provided by the National Natural Science Foundation of China (Nos. 62127901, 6207031149 and11903035).

Author contributions

Y. Bai proposed the idea and initiated the project. Y. Bai performed the theoretical analysis and rheological tests. Bai and Li analyzed the experimental data. Y. Bai and C. Yang wrote the manuscript. X. J. Zhang and X. Luo supervised the project. The manuscript was discussed and corrected by all the authors.

Conflict of interest

The authors declare that they have no conflict of interest.

Received: 24 February 2022 Revised: 24 June 2022 Accepted: 24 June 2022
Accepted article preview online: 29 June 2022
Published online: 06 July 2022

References

1. Harris, D. C. History of magnetorheological finishing. Proceedings of SPIE 8016, Window and Dome Technologies and Materials XII. Orlando: SPIE, 2011, 1-22.
2. Wan, S. L. et al. Novel magic angle-step state and mechanism for restraining the path ripple of magnetorheological finishing. *International Journal of Machine Tools and Manufacture* **161**, 103673 (2021).
3. Maloney, C. et al. Novel high-NA MRF toolpath supports production of concave hemispheres. Optifab, 2017, 1044806.
4. Bai, Y. et al. Rapid fabrication of a silicon modification layer on silicon carbide substrate. *Applied Optics* **55**, 5814-5820 (2016).
5. Kumar, M. et al. Magnetorheological method applied to optics

polishing: a review. *IOP Conference Series:Materials Science and Engineering* **804**, 012012 (2020).
6. Rolf, R. et al. Improving low, mid and high-spatial frequency errors on advanced aspherical and freeform optics with MRF. Third European Seminar on Precision Optics Manufacturing, 2016, 100090R.
7. Shorey, A. B. Mechanisms of material removal in magnetorheological finishing (MRF)of glass. PhD thesis, University of Rochester, Rochester, 2000.
8. Kordonski, V. & Golini, D. Progress update in magnetorheological finishing. Proceedings of the 6th International Conference on Electro-Rheological Fluid, Magnetorheological Suspensions and Their Applications. 1999, 2205-2212.
9. Shorey, A. B. et al. Experiments and observations regarding the mechanisms of glass removal in magnetorheological finishing. *Applied Optics* **40**, 20-33 (2001).
10. Lambropoulos, J. C., Jacobs, S. D. & Ruckman, J. Material removal mechanisms from grinding to polishing. *Ceramic Transactions* **102**, 113-128 (1999).
11. DeGroote, J. E. Surface interactions between nanodiamonds and glass in magnetorheological finishing (MRF). PhD thesis, University of Rochester, Rochester, 2009.
12. Miao, C. L. et al. Shear stress in magnetorheological finishing for glasses. *Applied Optics* **48**, 2585-2594 (2009).
13. Miao, C. et al. Frictional investigation for magnetorheological finishing (MRF) of optical ceramics and hard metals. Optical Fabrication and Testing 2008. Rochester: OSA, 2008.
14. Kordonski, W. & Gorodkin, S. Material removal in magnetorheological finishing of optics. *Applied Optics* **50**, 1984-1994 (2011).
15. Schinhaerl, M. et al. Calculation of MRF influence functions. Proceedings Volume 6671, Optical Manufacturing and Testing VII. San Diego: SPIE, 2007.
16. Schinhaerl, M. et al. Mathematical modelling of influence functions in computer-controlled polishing: part I. *Applied Mathematical Modelling* **32**, 2888-2906 (2008).
17. Liu, S. W. et al. Regionalized modeling approach of tool influence function in magnetorheological finishing process for aspherical optics. *Optik* **206**, 164368 (2020).
18. Jiang, J. et al. An experimental study on the normal stress of magnetorheological fluids. *Smart Materials and Structures* **20**, 085012 (2011).
19. Guo, C. Y. et al. An experimental investigation on the normal force behavior of magnetorheological suspensions. *Korea-Australia Rheology Journal* **24**, 171-180 (2012).
20. Wang, X. J. & Gordaninejad, F. Study of magnetorheological fluids at high shear rates. *Rheologica Acta* **45**, 899-908 (2006).
21. Cheal, O. & Ness, C. Rheology of dense granular suspensions under extensional flow. *Journal of Rheology* **62**, 501-512 (2018).
22. Rognon, P. G. et al. Dense flows of cohesive granular materials. *Journal of Fluid Mechanics* **596**, 21-47 (2008).
23. Chevoir F. et al. Friction law in dense granular flows. *Powder Technology* **190**, 264-268 (2009).
24. DeGiuli, E. & Wyart, M. Friction law and hysteresis in granular materials. *Proceedings of the National Academy of Sciences of the United States of America* **114**, 9284-9289 (2017).
25. Maurin, R., Chauchat, J. & Frey, P. Dense granular flow rheology in turbulent bedload transport. *Journal of Fluid Mechanics* **804**, 490-512 (2016).
26. Jop, P., Forterre, Y. & Pouliquen, O. A constitutive law for dense granular flows. *Nature* **441**, 727-730 (2006).
27. Salerno, K. M. et al. Effect of shape and friction on the packing and flow of granular materials. *Physical Review E* **98**, 050901(R) (2018).
28. De Vicente, J. et al. Squeeze flow magnetorheology. *Journal of Rheology* **55**, 753-779 (2011).
29. Guo, C. Y. et al. Compression behaviors of magnetorheological fluids under nonuniform magnetic field. *Rheologica Acta* **52**, 165-176 (2013).
30. Mokeev, A., Korobko, E. & Bubulis, A. Simulation of concentration distribution of dispersed particles of magnetorheological fluid in the gap workpiece-tool of finishing polishing device. *Mechanika* **20**, 221-225 (2014).